Numerical estimation of aircrafts' unsteady lateral-directional stability derivatives

N.L. Maričić [*]

Abstract

A technique for predicting steady and oscillatory aerodynamic loads on general configuration has been developed. The prediction is based on the Doublet-Lattice Method, Slender Body Theory and Method of Images. The chord and span wise loading on lifting surfaces and longitudinal bodies (in horizontal and vertical plane) load distributions are determined. The configuration may be composed of an assemblage of lifting surfaces (with control surfaces) and bodies (with circular cross sections and a longitudinal variation of radius). Loadings predicted by this method are used to calculate (estimate) steady and unsteady (dynamic) lateral-directional stability derivatives. The short outline of the used methods is given in [1], [2], [3], [4] and [5]. Applying the described methodology software DERIV is developed. The obtained results from DERIV are compared to NASTRAN examples HA21B and HA21D from [4]. In the first example (HA21B), the jet transport wing (BAH wing) is steady rolling and lateral stability derivatives are determined. In the second example (HA21D), lateral-directional stability derivatives are calculated for forward-swept-wing (FSW) airplane in antisymmetric quasi-steady maneuvers. Acceptable agreement is achieved comparing the results from [4] and DERIV.

Keywords: aerodynamics, lateral stability derivatives, directional stability derivatives

[*]Faculty of Technical Sciences, The Univesity of Prishtina. Kneza Miloša 7, 38220 Kosovska Mitrovica, Serbia, e-mail: maricicn@beotel.yu

1 Introduction

The idea to make use of the lifting surfaces' theories for estimation of aerodynamic derivatives was proposed [1], as the computer aerodynamics was just starting to develop. All the theories assume the linear-small amplitude, sinusoidal motion.

To the present day, especially for aircrafts' flutter calculations, numerous methods have been developed for accuracy unsteady aerodynamic loads determination. In this paper, the doublet-lattice finite element method is described and used. The chord wise and span wise load distribution on lifting surfaces and longitudinal z-vertical and y-lateral load distribution on bodies can be calculated for general configurations, using this method. The general configuration consists of an assemblage of lifting surfaces (with arbitrary plan form and dihedral, with or without control surfaces) and bodies (with variable circular cross sections).

In the flutter calculation for already known normal modes of the aircraft's structure, the unsteady load distributions on general configuration can be calculated. This possibility can be used to calculate (estimate) steady and unsteady stability aircraft's aerodynamic derivations. In this case, input data comprise a few of special rigid body motions of aircraft structure. A selection of these rigid body motions depends whether longitudinal or lateral-directional aircraft's aerodynamic derivatives are observed.

The software package UNAD had been developed for the calculation of unsteady aerodynamic forces of the general configuration for flutter calculation. The named package was modified and package DERIV has been developed for steady and unsteady longitudinal, lateral and directional aerodynamic derivative calculation of general configuration. The developed software DERIV was tested in [3] for longitudinal aerodynamic derivatives. Lateral-directional derivatives' test results from DERIV compared to the NASTRAN examples HA21B and HA21D are given in this paper.

According to the author's knowledge, software DERIV has been the first domastic package that can predict steady and unsteady derivatives based on the integration of unsteady aerodynamic loads over the whole aicraft's configuration.

2 Unsteady, subsonic aerodynamic loads

Aerodynamic finite element methods are based on matrix equation:

$$\{w\} = [A]\{\Delta Cp\} \quad ; \quad \Delta Cp = \frac{p_{lower} - p_{upper}}{\rho U^2/2} \tag{1}$$

In (1) $\{w\}$ is column matrix of downwashes (positive down), $[A]$ is square matrix of aerodynamic influence coefficients, and $\{\Delta Cp\}$ is column matrix of dimensionless lifting surface coefficient . The main flow is defined by density ρ and speed U of free stream. Aerodynamic elements are defined by general configuration geometry in the Cartesian coordinate system. The motion of general configuration is defined by degrees of freedom at aerodynamic grid points. Aerodynamic elements are trapezoidal boxes representing the lifting surfaces, ring slender bodies elements, and ring image elements representing slender body and interference influence.

The DLM is used for interfering lifting surfaces in subsonic flow. As DLM is based on the small-disturbance, linear aerodynamics, all lifting surfaces are assumed to lie nearly parallel to the main flow. Each interfering surface is divided into boxes. Boxes are small thick less (flat palate) trapezoidal lifting elements. The boxes are arranged to form strips. Strips lay parallel to free stream and the surface edges. Fold and hinge lines lie on the box boundaries. In order to reduce problem size, symmetry option is used. Unknown pressure ΔCp on each box is represented by a line of pressure doublet at quarter chord of the box. Known downwash w collocation (control) point lies at the mid span of the box three quarter chord. DLM aerodynamic elements are represented in Fig. 1.

The SBT is used to represent lifting characteristics for isolated bodies. SBT assumes that the flow near body is quasi-steady and two-dimensional. Bodies can have z-vertical, y-lateral or both degrees of freedom. Slender bodies of general configuration are divided slender body elements (axial velocity doublets) as shown in Fig. 2. Slender body elements are used to account aerodynamic loading due to the motion of the body.

The subsonic wing-body interference is based on the superposition of singularities and their images described in the method of images (MI). Each slender body is substituted by cylindrical interference body, which circumscribes the slender body. The interference body is divided in interference elements, as shown in Fig. 3. The interference element is used to
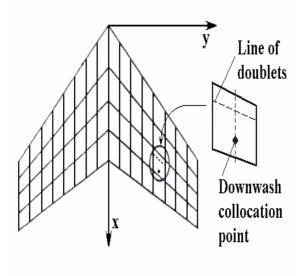
Figure 1: Lifting surface elements

include in calculation influence of other bodies and lifting surfaces on the body, to which element belongs. Each interference element is substituted by z-vertical and y-lateral modified acceleration potential pressure doublets. The primary wing-body interference is accounted for by a system of images of DLM vortices and a system of doublets within each interference element. There is no influence between two interference elements which belong to the same interference body.

Based on the above described, matrix relation (1) can be written in form:

$$
\left\{ \begin{array}{c} \bar{w}_w \\ 0 \\ \bar{w}_s \end{array} \right\} = \left\{ \begin{array}{ccc} A_{w,w} & A_{w,i} & A_{w,s} \\ A_{i,w} & A_{i,j} & A_{i,s} \\ 0 & 0 & A_{s,s} \end{array} \right\} \left\{ \begin{array}{c} \Delta C_p \\ \mu_i \\ \mu_s \end{array} \right\} \tag{2}
$$

In (2):

- $A_{r,s}$ is aerodynamic influence matrix element, which includes part of normal wash of unit strength r-the singularity on s-the finite element. Indices for the singularities and the aerodynamic finite elements are: w-lifting surface, i-image and s-slender body.
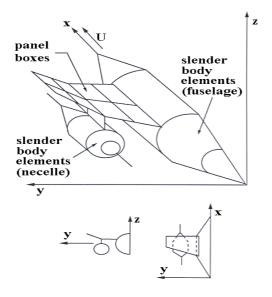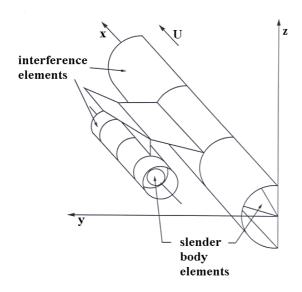
Figure 2: Slender body elements

Figure 3: Interference elements

- $\bar{w}_w$ is column of the known downwashes on lifting surface elements in the collocation (control) points normalized by free stream speed U.

- $\bar{w}_i = \{0\}$ is column of zero downwashes on the image elements.

- $\bar{w}_s$ is column of the known downwashes on the slender body elements in axis mid points normalized by free stream speed U.

- ΔCp is unknown column of the strengths of lifting surface singularities (acceleration potential pressure doublets).

- μ_i is unknown column of the strengths of images singularities (modified acceleration potential pressure doublets).

- μ_s is known column of the strengths of slender body singularities (velocity potential doublets).

The strength of slender body velocity potential doublet of unit length is known from two-dimensional theory. For j - the slender body element, described by midpoint (ξ, η, ζ) and radius R_j, follows:

$$\mu_{s,j}(\xi, \eta, \zeta, \omega) = 2\pi R_j^2 U \bar{w}_{s,j}(\xi, \eta, \zeta, \omega)$$

In the above relation ω is the angular frequency of the harmonically motion of slender body. As each slender body has z-vertical, y-lateral or both degrees of freedom, generally each j-the element of the body is substituted by the two velocity potential doublets, acting on the real element's axial length $\Delta \xi_j$:

$$\mu_{s,j}^{(y)} = 2\pi R_j^2 U \bar{w}_{s,j}^{(y)} \Delta \xi_j; \quad \mu_{s,j}^{(z)} = 2\pi R_j^2 U \bar{w}_{s,j}^{(z)} \Delta \xi_j \tag{3}$$

If boundary values on slender bodies are known, using (3) the strength of the slender bodies' singularities can be calculated. Substituting these obtained strengths in (2), it follows:

$$\left\{ \begin{array}{c} \bar{w}_w - \Delta\bar{w}_w \\ -\Delta\bar{w}_i \end{array} \right\} = \left[\begin{array}{cc} A_{w,w} & A_{w,i} \\ A_{i,w} & A_{i,i} \end{array} \right] \left\{ \begin{array}{c} \Delta Cp \\ \mu_i \end{array} \right\} \tag{4}$$

In (4), $\bar{w}_w - \Delta\bar{w}_w$ and $-\Delta\bar{w}_i$ are modification of normalized down washes on lifting surface elements and images caused by the known slender

body singularities. Relation (4) represents a system of linear equations with complex coefficients. The system can be solved in terms of the known boundary conditions for the unknowns ΔCp, $\mu_i^{(y)}$ and $\mu_i^{(z)}$.

Lifting surface pressure distribution ΔCp can be integrated to give the lifting surface contributions to the aerodynamic parameters of interest (aerodynamic coefficients, generalized forces, etc.).

The forces on the bodies are determined in more complicated manner. Every lifting surface box ΔCp, every image $\mu_i^{(y)}$ and $\mu_i^{(z)}$, every slender body axis doublet $\mu_s^{(y)}$ and $\mu_s^{(z)}$ affects the force distribution on bodies. It is known from unsteady computational aerodynamics that every singularity can be obtained from the point pressure doublet whose normal wash flow field is obtained from the standard lifting surfaces kernel K. Pressure coefficient $Cp(x, y, z)$ at point (x, y, z) on the body surface due to the point pressure doublet of the strength $\Delta Cp(\xi, \eta, \zeta)\Delta A$ in point (ξ, η, ζ) can be obtained by relation:

$$Cp(x, y, z) = \frac{\Delta Cp(\xi, \eta, \zeta)\Delta A}{4\pi} \quad e^{\iota\lambda Ma(x-\xi)} \frac{\partial}{\partial N}\left(\frac{e^{-\iota\lambda R}}{R}\right) \qquad (5)$$

In the above equation:

- Ma is free stream Mach number,

- $R^2 = (x - \xi)^2 + (1 - Ma^2)\left[(y - \eta)^2 + (z - \zeta)^2\right]$,

- $\lambda = \frac{\omega Ma}{U(1 - Ma^2)}$,

- $\vec{N}$ is unit vector in the direction of the doublet.

The term $\Delta Cp(\xi, \eta, \zeta)\Delta A$ is the total pressure doublet strength of lifting surface box of area ΔA in which lifting pressure coefficient is $\Delta Cp(\xi, \eta, \zeta)$. An equivalent point pressure doublet is assumed to act in $\frac{1}{4}$-mid chord box's point of lifting surface element. The finite length of body doublet $\Delta\xi$ is obtained by two point pressure doublets per each body element. The first is located at the leading edge of the element and has the strength $\mu e^{\frac{\iota\omega\Delta\xi}{2U}}$, and the second at the trailing edge of the strength $-\mu e^{-\frac{\iota\omega\Delta\xi}{2U}}$.

Equation (5) should be integrated over the whole body surface to obtain forces acting on the body due to point doublet located at (ξ, η, ζ).

The total force on the body should be sum of the all point pressure doublets effects. The detail integration of body force is given in [2].

At the end of analysis of unsteady, subsonic aerodynamic loads it is interesting to point out that unsteady aerodynamic loads of axis symmetric isolated slender body can be determined in elementary way, without using slender body velocity potential doublets. The element of axis symmetric slender body represents truncated cone of length dx and radius $R(x)$. From the momentum law, per example, in vertical direction the elementary lift force is:

$$dF_z(x) = \frac{D}{Dt}[\rho\pi R^2(x)w(x)dx] \tag{6}$$

In (6) $w(x)$ is small perturbation vertical upwash velocity and the operator $D(\cdots)/Dt$ is total derivative. The $R(x)$ is continual function up to the second derivative of the variable x. The operator $D(\cdots)/Dt$ for harmonical motion of slender body is defined by relation:

$$\frac{D(\cdots)}{Dt} = [U\frac{\partial}{\partial x} + \iota\omega](\cdots) \tag{7}$$

Subsituting (7) into (6) it follows:

$$\frac{dF_z(x)}{dx} = -\rho U^2 \left(\frac{\partial}{\partial x} + \iota\frac{k}{l}\right)\left(\pi R^2(x)\frac{w_z(x)}{U}\right) \tag{8}$$

In relation (8) $k = \omega l/U$ is reduced frequency, l reference length and $w_z(x) = -w(x)$ is vertical downwash velocity.

Let ΔCp_z be pressure coefficient acting in vertical direction on the element of slender body. Surface $2R(x)dx$, on which ΔCp_z acts is rectangle obtained as cross section of the slender body element and horizontal plane, containing axis of the element. In this case, lift (vertical) force on unit length of the slender body element is determined by relation:

$$dF_z(x) = \frac{\rho U^2}{2}\Delta Cp_z 2R(x)dx \quad \Rightarrow \quad \frac{dF_z(x)}{dx} = \rho U \Delta Cp_z R(x) \tag{9}$$

Equalizing (8) and (9) it can be obtained:

$$\Delta Cp_z = -\pi\left[2\bar{w}_z\frac{dR(x)}{dx} + R(x)\frac{d\bar{w}_z}{dx} + \iota\frac{k}{l}R(x)\bar{w}_z\right] \tag{10}$$

In (10) $\bar{w}_z = w_z/U$ is normalised downwash velocity.

If isolated slender body harmonically oscillates in vertical plane, its motion is described by relation:

$$h_z(x, y, z, t) = \Re e[h_{z_0}(x, y, z)e^{\iota\omega t}] \tag{11}$$

If down motion $h_z(x, y, z, t)$ is positive, then normalised downwash velocity on slender body is determined by relation:

$$\bar{w}_z = \frac{dh_{z_0}}{dx} + \iota\frac{k}{l}h_{z_0} \tag{12}$$

Substituting (12) into (10) it follows:

$$\Delta Cp_z = -\pi\left[\left(\frac{dR}{dx}\frac{dh_{z_0}}{dx} + \frac{R}{2}\frac{d^2h_{z_0}}{d^2x} - \frac{h_{z_0}^2}{2l^2}Rh_{z_0}\right)\right.$$
$$\left. +\iota\left(R\frac{dh_{z_0}}{dx} + h_{z_0}\frac{dR}{dx}\right)\right] \tag{13}$$

Based on (13) the distribution of unsteady vertical pressure coeficient on any isolated slender body can be determined.

Using the same procedure distribution of unsteady horizontal pressure coefficient ΔCp_y on isolated slender body generated by lateral (in horizontal plane) harmonic motion $h_y(x, y, z, t) = \Re e[h_{y_0}(x, y, z)e^{\iota\omega t}]$ can be obtained:

$$\Delta Cp_y = -\pi\left[\left(\frac{dR}{dx}\frac{dh_{y_0}}{dx} + \frac{R}{2}\frac{d^2h_{y_0}}{d^2x} - \frac{h_{y_0}^2}{2l^2}Rh_{y_0}\right)\right.$$
$$\left. +\iota\left(R\frac{dh_{y_0}}{dx} + h_{y_0}\frac{dR}{dx}\right)\right] \tag{14}$$

Vertical and lateral aerodynamic force on j - the isolated slender body element of length $\Delta\xi_j$ and radius $R_j(x_j, y_j z_j')$ in its midpoint is:

$$F_{z_j} = \rho U^2\Delta Cp_{z_j}R_j\Delta\xi_j \quad ; \quad F_{y_j} = \rho U^2\Delta Cp_{y_j}R_j\Delta\xi_j \tag{15}$$

New developed relations (6) to (15) for calculation of unsteady, subsonic aerodynamic loads on axis symmetric isolated slender body can be used to control the same loads obtained from concept of velocity potential doublets.

3   Short theoretical aproach

Dynamic lateral-directional aerodinamic derivateves of an aircraft are:

- lateral force derivatives:

$$C_{y\beta}, \quad C_{yp}, \quad C_{yr}, \quad C_{y\delta_a}, \quad C_{y\delta_r}, \quad C_{y\dot{\beta}}, \quad C_{y\dot{p}}, \quad C_{y\dot{r}},$$

- roll moment derivatives:

$$C_{l\beta}, \quad C_{lp}, \quad C_{lr}, C_{l\delta_a}, \quad C_{l\delta_r}, \quad C_{l\dot{\beta}}, \quad C_{l\dot{p}}, \quad C_{l\dot{r}}, \qquad (16)$$

- jaw moment derivatives:

$$C_{n\beta}, \quad C_{np}, \quad C_{nr}, \quad C_{n\delta_a}, \quad C_{n\delta_r}, \quad C_{n\dot{\beta}}, \quad C_{n\dot{p}}, \quad C_{n\dot{r}}.$$

In relations (16) β is sideslip angle of aircraft flying with speed U, defined in Fig. 4.
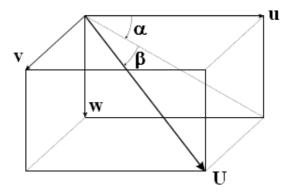

Figure 4: Sideslip angle

If v is lateral component of U, then based on Fig. 4. slip angle is:

$$\sin\beta = \frac{v}{U}$$

Differenting upper relation with respect to v gives:

$$\cos\beta\frac{\partial\beta}{\partial v} = \frac{1}{U} - \frac{v^2}{U^3} = \frac{1}{U}\cos^2\beta$$

For small perturbation from nominal flight, it follows:

$$\frac{\partial \beta}{\partial v} \approx \frac{1}{U}$$

Thus, β and v are directly proportional when operating near nominal flight condition.

Value p is the rate of aircraft's roll (Fig. 5.) in body fixed coordinate system $X_b Y_b Z_b$. If θ is bank angle $p = d\theta/dt$.
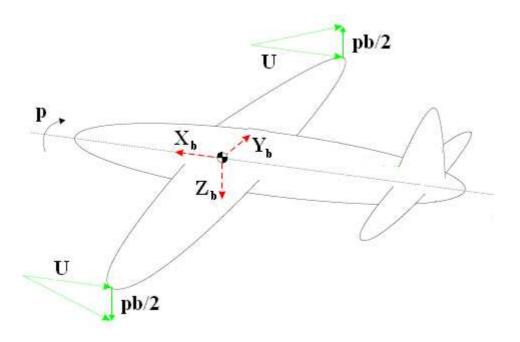

Figure 5: Roll rate

Value r is the rate of aircraft's jaw (Fig. 6.) in body fixed coordinate system $X_b Y_b Z_b$ and if ψ is jaw angle, it follows $r = d\psi/dt$.

In calculation of the dynamic lateral-directional derivatives reference length l is usually wing semispan $b/2$. The total reference sideslip angle β_m can be obtained as a linear combination of all involved kinematic effects:

$$\beta_m = \beta_{m\beta}\beta + \beta_{m\delta_a}\delta_a + \beta_{m\delta_r}\delta_r + \beta_{mp}\frac{pb}{2U} + \beta_{mr}\frac{rb}{2U} +$$
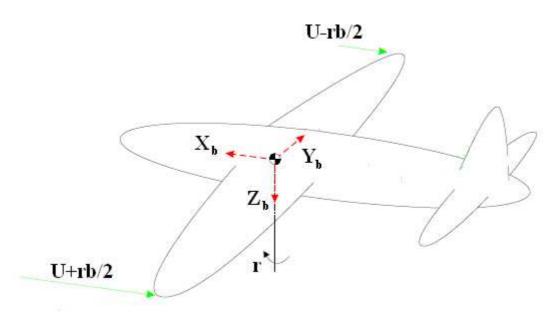
Figure 6: Jaw rate

$$+\beta_{m\ddot{y}}\frac{\ddot{y}}{g} + \beta_{m\dot{p}}\frac{\dot{p}b}{2U} + \beta_{m\dot{r}}\frac{\dot{r}b}{2U} + \cdots \tag{17}$$

In (16) and (17) influences of antisymmetric aileron deflection $\delta_a = (|\delta_a^{right}| + |\delta_a^{left}|)/2$ and antisymmetric rudder deflections $\delta_r = (|\delta_r^{right}| +|\delta_r^{left}|)/2$ (if two rudders are located on fins out of aircraft symmetry plane) are involved in calculation of steady lateral-directional derivatives. . It should be mentioned that the aerodynamic forces on control surfaces strongly depend on their boundary layers. As in the used methods viscosity effects are neglected, derivatives with respect to δ will give only trends to accurate values.

Generally speaking, aerodynamic stability derivatives are determined in body fixed axis (stability) system $X_bY_bZ_b$, while aerodynamic forces and moments are calculated aerodynamic axis system $X_aY_aZ_a$. The aerodynamic system is colinear with velocity coordinate system $X_vY_vZ_v$. The axis of aerodynamic system are opposite to the axis of velocity system $(x_a = -x_v; \quad y_a = -y_v; \quad z_a = -z_v)$, when the motion of aircraft is in a straight line. All of the three systems have the same origin in the center of gravity C_{cg} of aircraft structure. Used coordinate systems are represented

in Fig. 7. In connection with relation (16), it is necessary to outline that
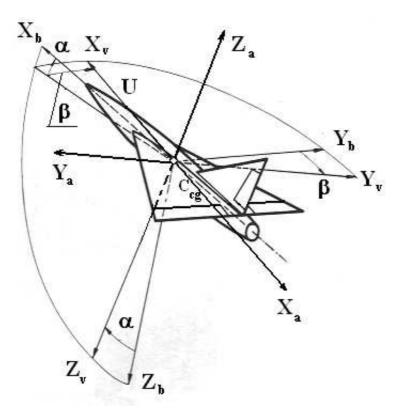$C_{y_v} = -C_{y_a}$.

Figure 7: Coordinate systems used

In the reference condition the Y_a- axis is normal to airspeed U, but departs from it, Y_b- axis is moving with the airplane during a disturbance. That means that the sideslip angle β_s, defined as the angle between the X_b- axis and the direction normal to U, is not necessarily identical to the absolute value of the sideslip angle $\beta_a = \beta$, used in aerodynamic calculations. The axis Y_a is in direction normal to the undisturbed flight path, while - axis is oscillating with rigid airplane. Clearly, β_s represents the disturbance from an aerodynamic state β. As small disturbances have been assumed, simple conversion rules between the stability and the aerodynamic axis systems for antisymmetric motions are:

$$X_b Y_b Z_b \quad \Rightarrow \quad \beta \quad = \quad \iota \frac{\omega}{U} h_y - \psi \quad \Leftarrow \quad X_a Y_a Z_a$$

$$X_b Y_b Z_b \quad \Rightarrow \quad p \quad = \quad \iota \omega \theta \quad \Leftarrow \quad X_a Y_a Z_a$$

$$X_b Y_b Z_b \quad \Rightarrow \quad r \quad = \quad \iota \omega \psi \quad \Leftarrow \quad X_a Y_a Z_a$$

In the above relations h_y is lateral translation, θ is roll angle, ψ is jaw angle and ω is angular frequency of harmonic motion of an aircraft.

In the stability axis system β_s - variation is equivalent to a variation of lateral wash of the airplane. So, it is equivalent to the sideslip angle to be prescribed in the methods used in this paper, where the aerodynamic axis system is used. The roll rate p, as defined in the stability axis system in Fig. 5., is felt by the airplane as linearly, span wise varying normal wash around the mass center of aircraft in $Y_b C_{cg} Z_b$ system. In the same way the jaw rate r is defined in Fig. 6. in $X_b C_{cg} Y_b$ system.

As said in the introduction of this paper, the concept of integration of unsteady aerodynamic loads is used, so obtained side force $\bar{C}_y$, roll moment $\bar{C}_l$ and jaw moment $\bar{C}_n$ coefficients are complex numbers

In order to calculate lateral-directional derivatives, five cases of motion of general configuration $\{h_j(x, y, z, t) = h_{0_j}(x, y, z) \Re e(e^{\iota \omega t}), j = 1, (1), 5\}$, are of interest.

The first two cases are connected to steady lateral-directional derivatives caused by aileron and rudder deflections $\{h_j(x, y, z, t) = h_{0_j}(x, y, z), j = 1, (1), 2\}$. The last three of them are related to quasi-steady lateral-directional harmonic motions $\{h_j(x, y, z, t) = h_{0_j}(x, y, z) \Re e(e^{\iota \omega t}), j = 3, (1), 5\}$: lateral translation, roll and jaw of the general configuration. From boundary conditions of these five rigid body modes one can determine appropriate aerodynamic load distributions and by integration of these loads over the whole aircraft outer surface in (16) named derivatives. It is known from the flutter calculation that boundary conditions can be obtained from aircraft's structure normal modes' shapes (deflections and slopes of mode shape), as normalized downwash on each lifting surface or body's element is:

$$\bar{w}_{i_j} = \frac{w_{i_j}}{U} = \frac{dh_{0_j}}{dx} + \frac{1}{U}\frac{dh_{0_j}}{dt} = \frac{dh_{0_j}}{dx} + \iota\frac{\omega}{U}h_{0_j} = \frac{dh_{0_j}}{dx} + \iota\frac{k}{l_{ref}}h_{0_j}; \quad k = \frac{\omega l_{ref}}{U}$$
(18)

In relation (18), the index j is the number of element, the index i is the normal mode number and l_{ref} is in calculation reference length.

Steady lateral-directional derivatives as function of aileron and rudder deflections can be determined for these two steady cases:

- Mode 1 – Steady ailerons' deflection

  The default antisymmetric aileron deflection is $\delta_a = 0.1$. Only lifting surface elements on the wing's ailerons are deflected. In any aileron control point (x_{kj}, y_{kj}, z_{kj}) it follows:

  $$h_{0_1} = \delta_a(x_{kj} - x_{k,a}^{arm})\cos\lambda_a \quad ; \quad \bar{w}_1 = \frac{\partial h_{0_1}}{\partial x} = \delta_a\cos\lambda_a \qquad (19)$$

  In (19), $x_{k,a}^{arm}$ is normal distance from control point to aileron rotation axis and λ_a is the swept angle of aileron rotation axis. On all the other elements, meaning all the other lifting surface elements and image bodies elements $h_{0_1} = 0$ and $\frac{\partial h_{0_1}}{\partial x} = 0$.

- Mode 2 – Steady rudders' deflection

  The default antisymmetric rudder deflection is $\delta_r = 0.1$. Only lifting surface elements on the fin's rudder are deflected. In any rudder control point (x_{kj}, y_{kj}, z_{kj}) it follows:

  $$h_{0_2} = \delta_r(x_{kj} - x_{k,r}^{arm})\cos\lambda_r \quad ; \quad \bar{w}_2 = \frac{\partial h_{0_2}}{\partial x} = \delta_r\cos\lambda_r \qquad (20)$$

  In (20), $x_{k,r}^{arm}$ is normal distance from control point to rudder rotation axis and λ_r is the swept angle of rudder rotation axis. On all other elements, meaning all the other lifting surface elements and image bodies elements $h_{0_2} = 0$ and $\frac{\partial h_{0_2}}{\partial x} = 0$.

Quasi-steady antisymmetric motions of general configuration significant for lateral-directional derivatives are lateral translation, roll and jaw:

- Mode 3 – Quasi-steady lateral translation

  Let general configuration harmonically oscillate as $h_{n_3} = h_{0_3} \Re e(e^{\iota \omega t})$ in lateral direction and amplitude of lateral motion is constant and equal $h_{0_3} = 0.1 \frac{l_{mac}}{2}$. In this case it follows:

  $$\bar{w}_3 = \frac{\partial h_{0_3}}{\partial x} + \iota \frac{\omega}{U} h_{0_3} = 0.1 \iota \frac{\omega l_{mac}}{2U} = 0.1 \frac{\iota k}{2} \quad ; \quad k = \frac{\omega l_{mac}}{U} \qquad (21)$$

  In relation (21) $l_{ref} = l_{mac}$ is mean aerodynamic chord of general configuration (usually wing). In any j - the element of general configuration discretisation with dihedral angle

  γ_j from relation (21) it follows:

  $$h_{0_3}(x_{kj}, y_{kj}, z_{kj}) = 0.1 \frac{l_{mac}}{2} sin\gamma_j; \quad \frac{\partial h_{0_3}(x_{kj}, y_{kj}, z_{kj})}{\partial x} = 0$$

- Mode 4 – Quasi-steady roll

  Slow harmonic roll of general configuration around its longitudinal body fixed axis is defined over harmonic oscillation of bank angle $\theta(t) = \theta_0 \Re e(e^{\iota \omega t})$. Roll rate is defined as:

  $$p(t) = \frac{d\theta(t)}{dt} \equiv \dot{\theta} \quad = \iota \omega \theta(t) \quad \Rightarrow \quad p = \iota \omega \theta_0 \qquad (22)$$

  For $\theta_0 = .1$ from (22) it follows:

  $$\frac{pb}{2U} = \iota \frac{\omega b}{2U} \theta_0 = 0.1 \iota k \quad ; \quad l_{ref} = \frac{b}{2} \qquad (23)$$

  Using (23) normalised velocity $\bar{w}_4$ in any point on lifting system (d_y normal distance from the selected point to X_b axis) generated by rigid body, quasi-steady, harminic roll generally can be defined as

  $$\bar{w}_4 = \frac{pd_y}{U} = \frac{pb}{2U} \frac{2}{b} d_y = \iota k \frac{0.2}{b} d_y \qquad (24)$$

In any control point (x_{kj}, y_{kj}, z_{kj}) from relations (18) and (24) it follows:

$$h_{0_4}(x_{kj}, y_{kj}, z_{kj}) = \frac{0.2}{b}\sqrt{y_{kj}^2 + (z_{kj} - z_{cg})^2}\cos(\vartheta_j - \gamma_j); \quad \frac{\partial h_{0_4}}{\partial x} = 0 \tag{25}$$

In relation (25) γ_j is dihedral angle of $j-the$ element of discretisation of general configuration and ϑ_j follows from relation:

$$\vartheta_j = \arctan\frac{z_j - z_{cg}}{y_j}$$

- Mode 5 – Quasi-steady jaw

  Slow harmonic jaw of general configuration around its vertical body fixed axis is defined over harmonic oscillation of jaw angle $\psi = \psi_0\Re e(e^{\iota\omega t})$. Jaw rate is defined as:

$$r(t) = \frac{d\psi(t)}{dt} \equiv \dot{\psi} \quad = \iota\omega\psi(t) \quad \Rightarrow \quad r = \iota\omega\psi_0 \tag{26}$$

For $\frac{rb}{2U} = 0.1$ from (26) it follows:

$$\frac{rb}{2U} = \frac{\dot{\psi}b}{2U} = 0.1 \quad \Rightarrow \quad \frac{r}{U} = \frac{\dot{\psi}}{U} = \frac{0.2}{b} \tag{27}$$

Based on (26) and (27) general configuration jaw angle can be obtained:

$$\frac{dh_{0_5}(x)}{dx} = \psi_0(x) \equiv \frac{\dot{\psi}}{U}(x - x_{cg})\sin\gamma_j = \frac{0.2}{b}(x - x_{cg})\sin\gamma_j$$

$$h_{0_5} = \frac{0.2}{b}\sin\gamma_j\int(x - x_{cg})dx = \frac{0.2}{b}\sin\gamma_j\left(\frac{x^2}{2} - x_{cg}x + C\right) \tag{28}$$

Constant C in (28) can be determined using boudary condition in the centar of gravity of general configuration:

$$x = x_{cg} \text{ and } h_{0_5}(x = x_{cg}) = 0 \quad \Rightarrow \quad C = \frac{x_{cg}^2}{2} \tag{29}$$

From (28) and (29) it can be obtained:

$$h_{0_5} = \frac{0.1}{b}(x - x_{cg})^2 \sin \gamma_j; \quad \frac{dh_{0_5}}{dx} = \frac{0.2}{b}(x - x_{cg}) \sin \gamma_j \qquad (30)$$

In any control point (x_{kj}, y_{kj}, z_{kj}) from relation (30) it follows:

$$h_{0_5}(x_{kj}, y_{kj}, z_{kj}) = \frac{0.1}{b}(x_{kj} - x_{cg})^2 \sin \gamma_j$$

$$\frac{dh_{0_5}(x_{kj}, y_{kj}, z_{kj})}{dx} = \frac{0.2}{b}(x_{kj} - x_{cg}) \sin \gamma_j$$

The previous three quasi-steady motions should be understood as unsteady harmonic aircraft motions characterising that their reduced frequences converge to zero $k = \frac{\omega l}{2U} \to 0$.

For analysed five cases of motion appropriate aerodynamic loads distribution can be obtained. In the first two cases, as steady conditions are involved, load distributions are real numbers. In the last three cases, quasi-steady motions are analysed, so load distributions are complex numbers.

Generally speaking, aerodynamic coefficients of side force, rolling and jawing moment can be represented over lateral-directional derivatives based on the development in the MacLaurent series:

$$C_y = C_{y_\beta}\beta + C_{y_p}\frac{pb}{2U} + C_{y_r}\frac{rb}{2U} + C_{y_{\delta_a}}\delta_a + C_{y_{\delta_r}}\delta_r +$$

$$C_{y\dot\beta}\frac{\dot\beta b}{2U} + C_{y\dot p}\frac{\dot p b}{2g} + C_{y\dot r}\frac{\dot r b}{2g} + \cdots$$

$$C_l = C_{l_\beta}\beta + C_{l_p}\frac{pb}{2U} + C_{l_r}\frac{rb}{2U} + C_{l_{\delta_a}}\delta_a + C_{l_{\delta_r}}\delta_r +$$

$$C_{l\dot\beta}\frac{\dot\beta b}{2U} + C_{l\dot p}\frac{\dot p b}{2g} + C_{l\dot r}\frac{\dot r b}{2g} + \cdots$$

$$C_n = C_{n_\beta}\beta + C_{n_p}\frac{pb}{2U} + C_{n_r}\frac{rb}{2U} + C_{n_{\delta_a}}\delta_a + C_{n_{\delta_r}}\delta_r +$$

$$C_{n\dot{\beta}}\frac{\dot{\beta}b}{2U} + C_{n\dot{p}}\frac{\dot{p}b}{2g} + C_{n\dot{r}}\frac{\dot{r}b}{2g} + \cdots$$

For steady cases, using direct integration od aerodynamic loads and appropriate normalisation steady lateral-directional derivatives dependent to δ_a and δ_r can be obtained.

For unsteady cases, by appropriate summing of known aerodynamic loads set of side force, moment of roll and jaw coefficients would be calculated for small reduced frequency ($k = 0.01 \div 0.1$):

$$\{[\bar{C}_y(j); \bar{C}_l(j); \bar{C}_n(j)], \quad j = 3, (1), 5\} \tag{31}$$

Based on (31) lateral-directional derivatives due to sideslip angle β and rate of sideslip angle $\dot{\beta}$ can be determined:

$$C_{y_\beta} = \frac{1}{k}\Im m[\bar{C}_y(3)] = -\Re e[\bar{C}_y(5)]; \quad C_{y_{\dot{\beta}}} = -\frac{1}{k^2}\Re e[\bar{C}_y(3)]$$

$$C_{l_\beta} = \frac{1}{k}\Im m[\bar{C}_l(3)] = -\Re e[\bar{C}_l(5)]; \quad C_{l_{\dot{\beta}}} = -\frac{1}{k^2}\Re e[\bar{C}_l(3)]$$

$$C_{n_\beta} = \frac{1}{k}\Im m[\bar{C}_n(3)] = -\Re e[\bar{C}_n(5)]; \quad C_{n_{\dot{\beta}}} = -\frac{1}{k^2}\Re e[\bar{C}_n(3)]$$

In the same way lateral-directional derivatives of roll can be obtained:

$$C_{y_p} = \frac{1}{k}\Im m[\bar{C}_y(4)]; \quad C_{y_{\dot{p}}} = -\frac{1}{k^2}\Re e[\bar{C}_y(4)]$$

$$C_{l_p} = \frac{1}{k}\Im m[\bar{C}_l(4)]; \quad C_{l_{\dot{p}}} = -\frac{1}{k^2}\Re e[\bar{C}_l(4)]$$

$$C_{n_p} = \frac{1}{k}\Im m[\bar{C}_n(4)]; \quad C_{n_{\dot{p}}} = -\frac{1}{k^2}\Re e[\bar{C}_n(4)]$$

Based on kinematics motions of any rigid body in slip, jaw and lateral translation are connected in horizontal plane over relation:

$$\beta(t) + \psi(t) = \frac{1}{U}\frac{dh_3}{dt} \tag{32}$$

If rigid body oscillates harmonically from (32) it follows:

$$\beta_0 + \psi_0 = \iota \frac{\omega}{U} h_{3_0} \tag{33}$$

It is clear from (33) and (21) that amplitude of quasi-steady jaw angle ψ_0 can be determined using relation:

$$\psi_0 = \iota \frac{k}{l_{mac}} h_{3_0} - \beta_0 \tag{34}$$

Using relation (34) it follows:

$$C_{y_r} = \frac{1}{k} \left\{ \Im m[\bar{C}_y(5)] - \frac{\Re e[\bar{C}_y(3)]}{k} \right\} ;$$

$$C_{y_{\dot r}} = \frac{1}{k^2} \left\{ \Re e[\bar{C}_y(5)] + \frac{\Im m[\bar{C}_y(3)]}{k} \right\} ;$$

$$C_{l_r} = \frac{1}{k} \left\{ \Im m[\bar{C}_l(5)] - \frac{\Re e[\bar{C}_l(3)]}{k} \right\} ;$$

$$C_{l_{\dot r}} = \frac{1}{k^2} \left\{ \Re e[\bar{C}_l(5)] + \frac{\Im m[\bar{C}_l(3)]}{k} \right\} ;$$

$$C_{n_r} = \frac{1}{k} \left\{ \Im m[\bar{C}_n(5)] - \frac{\Re e[\bar{C}_n(3)]}{k} \right\} ;$$

$$C_{n_{\dot r}} = \frac{1}{k^2} \left\{ \Re e[\bar{C}_n(5)] + \frac{\Im m[\bar{C}_n(3)]}{k} \right\} .$$

4   Examples

Two examples, HA21B and HA21D, from the well known software NAS-TRAN [4] are tested. Case HA21B is used for checking steady lateral (roll) aerodynamic derivatives and case HA21D for testing unsteady lateral-directional derivatives.

4.1 Example HA21B

The first example is jet transport wing known as BAH wing. The geometry of BAH wing is taken from [6] pp. 45 and shown on Fig. 8. The wing root chord is $c_r = 225[in] = 5.715[m]$, tip chord $c_t = 100[in] = 2.54[m]$ and total span $b = 1000[in] = 25.4[m]$. The per side wing area is $A = 81250[in^2] = 52.41925[m^2]$ and reference chord $l_{mac} = 170.5[in] = 4.3310[m]$. In [4] reference chord is taken as $l_{mac} = 162.5[in] = 4.1275[m]$ due to wing tip curvilinear ending.
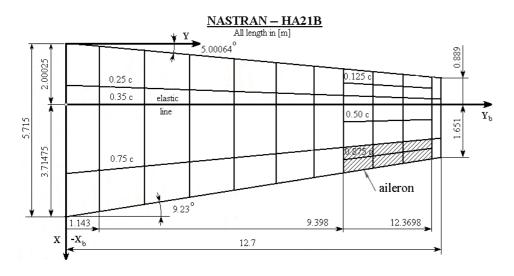

Figure 8: Idealization of BAH configuration

The BAH wing, idealised as half-span wing/aileron combination, is divided into three parts with total 42 panels, 6 of which are on the aileron. The idealisation is shown in Fig. 8. The part between the centerline and the aileron is divided into 7 span wise strips with 3 unequal stream wise panels. The width of the first strip is given on Fig. 8. and the next 6 strips characterize equal width. The part containing the aileron is specified by 3 equal strips and 6 unequal panels. The part between the aileron and wing tip is divided into 1 strip with 3 unequal panels. The strips' division on panels is defined on Fig. 8.

Wing is tested in steady roll, at the sea level and on low Mach number $Ma = 0.01$. If wing is restrained rolling moment is defined as:

$$C_l = +C_{l_p}\frac{pb}{2U} + C_{l_{\dot{p}}}\frac{\dot{p}b}{2g}$$

In unrestrained condition inertial derivative $C_{l_{\dot{p}}}$ vanishes and its effect is included in the other two derivatives.

Parallel results from DERIV and NASTRAN are shown in Table 1. Notation *ldd* in Table 1. means lateral-directional derivative.

ldd	[4]	DERIV
$C_{l_{\delta_\alpha}}$		-0.5262
C_{l_p}	-0.5193	-0.5262
$C_{l_{\dot{p}}}$	-0.0002	-0.0003

Table 1: Case HA21B results

Based on Table 1. the results from DERIV and NASTRAN are in good agreement.

4.2   Example HA21D

The case is taken from [4]. Forward-Swept-Wing (FSW) airplane with coplanar canard and fin was tested at trimmed sea level steady flight on Mach number $Ma = 0.9$. The model is idealized as shown in Fig. 9.

The wing has an aspect ratio 4.0, no taper, twist, camber, or incidence relative to fuselage, and forward sweep angle 30^0. The canard has an aspect ratio 1.0, and no taper, twist, camber, incidence, or sweep. The fin has an aspect ratio 2.0, and no taper, twist, camber or incidence and backward sweep angle 30^0. All chords of the wing, the canard and the fin are constant and equal to $3.05[m]$. The reference length of the configuration is equal to the wing mean aerodynamic chord $l_{mac} = 3.05[m]$. The half-span model of aircraft is divided into 32 equal panels (8 span-wise, 4 chord-wise) on the wing, 8 equal panels (2 span-wise, 4 chord-wise) on the canard and 16 equal panels (4 span-wise, 4 chord-wise) on the fin.

Location and idealization of aileron and rudder is shown in Fig. 9. The chords of aileron and rudder are quarter length of the belonging wing and fin chord. Aileron is expanding from mid to the tip of the wing, and rudder is propagating from the whole fin span.
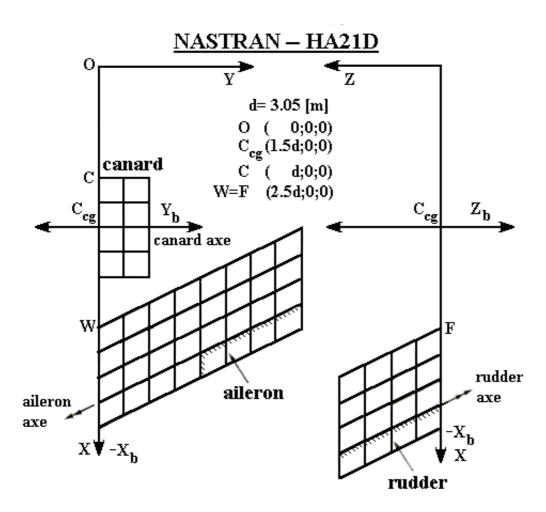
NASTRAN – HA21D

d= 3.05 [m]

O (0;0;0)
C_{cg} (1.5d;0;0)
C (d;0;0)
W=F (2.5d;0;0)

canard

canard axe

aileron

aileron
axe

aileron
axe

rudder
axe

rudder

Figure 9: Idealization of FSW configuration

The fuselage length is 9.150 $[m]$. Aerodynamic forces on the fuselage are neglected.

The aerodynamic coordinate system is located in the beginning of the fuselage in coplanar plane of wing-canard. Center of gravity is 4.575$[m]$ behind aerodynamic coordinate system origin in midpoint of canard root-chord.

Geometry and aerodynamic idealization of FSW configuration is given in Fig. 9. The configuration center of gravity, significant for directional derivatives, is shown on the same figure.

Comparative results from softwares NASTRAN and DERIV are given in Table 2. Notation *ldd* in Table 2. means lateral-directional derivative. The results in Table 2. marked as (∗) were not available in [4].

Based on the results given in Table 2. unsteady lateral-directional aerodynamic derivatives from NASTRAN and DERIV are in acceptable agreement.

5   Conclusions

A concise overview of the developed numerical procedure and test results of new software DERIV, for calculation of lateral-directional aerodynamic derivatives for general configurations, is given in the paper. New, useful relations are developed for calculation of unsteady, subsonic aerodynamic loads on an axis symmetric isolated slender body. These relations can be used to verify the same loads obtained from the concept of velocity potential doublets.

The contributions in the described research can be seen in the detailed numerical development of the selected method and in development and testing of the software DERIV.

The developed software DERIV is tested in NASTRAN cases HA21B and HA21D. The obtained results from DERIV are in acceptable agreement to NASTRAN.

In the future, DERIV software should be tested in cases from the engineering practice.

ldd	[4]	DERIV
C_{y_β}	-0.7147	-0.7159
$C_{y_{\dot\beta}}$	$(*)$	-0.0781
$C_{y_{\delta_a}}$	-0.1082	-0.1127
$C_{y_{\delta_r}}$	$+0.3491$	$+0.3672$
C_{y_p}	$+0.0797$	$+0.0692$
$C_{y_{\dot p}}$	$+0.0018$	$+0.0013$
C_{y_r}	$+0.7233$	$+0.7315$
$C_{y_{\dot r}}$	-0.0237	-0.0264
ldd	[4]	DERIV
C_{l_β}	-0.0369	-0.0348
$C_{l_{\dot\beta}}$	$(*)$	-0.0120
$C_{l_{\delta_a}}$	$+0.2748$	$+0.2834$
$C_{l_{\delta_r}}$	$+0.0375$	$+0.0392$
C_{l_p}	-0.4184	-0.4031
$C_{l_{\dot p}}$	-0.0002	-0.0004
C_{l_r}	$+0.0430$	$+0.0464$
$C_{l_{\dot r}}$		-0.0001
ldd	[4]	DERIV
C_{n_β}	$+0.2588$	$+0.2599$
$C_{n_{\dot\beta}}$	$(*)$	$+0.0163$
$C_{n_{\delta_a}}$	$+0.0395$	$+0.0419$
$C_{n_{\delta_r}}$	-0.1707	-0.1772
C_{n_p}	-0.0261	-0.0247
$C_{n_{\dot p}}$	-0.0003	-0.0002
C_{n_r}	-0.2775	-0.2809
$C_{n_{\dot r}}$	$+0.0004$	$+0.0016$

Table 2: Case HA21D results

References

[1] Etkin, B., Reid, L., *Dynamics of Flight: Stability and Control,* Jonh Wiley and Sons., New York, NY, third edition, 1996.

[2] Rodden, W., Johnson, E., *MSC/NASTRAN Aeroelastic User's Guide,* Version 68, The MacNeal-Schwendler Corp., 1994.

[3] Maričić, N., *Software Development for Subsonic Aircraft's Unsteady Longitudinal Stability Derivatives*, Theoret. Appl. Mech., Vol. 32, No. 4, 2005., pp. 319-340.

[4] Bellinger, E., *MSC/NASTRAN Handbook for Aeroelastic Analysis*, Vol. 2., Version 65, The MacNeal-Schwendler Corp., 1987.

[5] MSC Software Corp. *NEWPAN - MSC.NASTRAN^{TM} AEROELASTIC*, 2004.

[6] Bisplinghoff, R., Ashley, H., Halfman, R., *Aeroelasticity,* Addison-Wesley Publishing Company, Cambrige, Mass., 1942.

[7] Green, L.,Spence, A.,Murphy, P, *Comutational Methods for Dynamic Stability and Control Derivatives*, AIAA 2004-0015, 2004.

Numerička procena nestacionarnih poprečnosmernih derivativa stabilnosti aviona

UDK 536.7

Nestacionarni poprečnosmerni aerodinamički derivativi subsoničnih aviona proizvoljne konfiguracije mogu se numerički proceniti korišćenjem metoda konačnih elemenata baziranih na metodi rešetke dipola (Doublet Lattice Method - DLM), teorije vitkih tela (Slender Body Theory - SBT) i metodi zamene (Method of Images - MI). Primenom navedenih metoda razvijen je postupak proračuna raspodela stacionarnih i oscilatornih aerodinamičkih opterećenja aviona. Raspodele aerodinamičkih opterećenja po uzgonskim površinama definisane su u pravcu tetiva i razmaha, a raspodele po telima u vertikalnoj i bočnoj ravni koje sadrže osu simetrije tela. Konfiguraciju aviona može da sačinjava proizvoljan skup uzgonskih površina (uključujući komandne površine) i proizvoljan skup tela kružnog poprečnog preseka promenjivog duž ose simetrije tela. Kratak pregled korišćenih metoda dat je u [1], [2], [3], [4] i [5]. Na bazi navedenih metoda razvijen je softverski paket DERIV. Rezultati dobijeni programom DERIV testirani su na primerima HA21B i HA21D iz NASTRAN-a datih u [4]. U prvom primeru (HA21B) za krilo mlaznog transportnog aviona (BAH krilo), koje stacionarno rotira oko podužne ose aviona, odredjeni su derivativi valjanja. U drugom primeru (HA21D) izračunati su poprečnosmerni derivativi konfiguracije sa kanardom i krilom koje ima strelu unapred (FSW konfiguracija). Konfiguracija osciluje kvazistacionarno i antisimetrično. Postignuto je prihvatljivo slaganje uporednih rezultata iz [4] i programa DERIV.